Microwave Surface Impedances of BCS Superconducting Thin Films

Chien-Jang Wu and Tseung-Yuen Tseng, *Senior Member, IEEE*

***Abstract*— The microwave propagation-dominated problem in the multilayer structure made of a BCS superconducting film and a dielectric substrate is investigated theoretically by using the modified two-fluid model and transmission line theory. The effective microwave surface impedances are studied as functions of temperature, frequency, and film thickness, as well as substrate thickness. Special attention is paid to the substrate resonance phenomenon in the resonant structure. The influence of BCS coherence effects on surface impedance and resonant behavior is clearly demonstrated. The resonant effect in the stack structure is well interpreted with the help of the transverse resonance technique in the microwave theory.**

I. Introduction

STUDIES of electromagnetic microwave responses of superconductors are of paramount importance and are extensively used to investigate the fundamental physics of both conventional and high-T_c superconductors. Measurements of surface impedance $Z_s = R_s + jX_s$ also provide a great deal of information about electronic conduction mechanism. On the two-fluid model basis, the surface resistance R_s reflects the loss in the superconductor, which is connected with the fraction of unpaired conduction electrons; whereas, the surface reactance X_s is directly proportional to penetration depth. The surface impedance is also a key parameter in the microwave applications, such as filters, resonators, and delay lines. The performance and dissipation of these passive microwave devices are closely related to the surface resistances of superconductors. Experiments are usually performed on superconducting thin films deposited on various substrates in the microwave regime. The surface impedance of such system is thus referred to as the so-called effective surface impedance which relies on the film thickness as well as the material properties of the dielectric substrates. Furthermore, as the film thickness is of the order of the penetration depth, the magnitude of the effective surface impedance is strongly enhanced.

The microwave propagation-dominated problem of such a multilayer structure has been investigated both experimentally and theoretically [1]–[7]. In these studies, all efforts were made primarily on the high-T_c superconducting films, the $YBa_2Cu_3O_{7-x}$ system. The very interesting finding was the observation of oscillation behavior in the normal-state effective surface resistance [1]–[4]. Another feature also of note was the resonance phenomenon in stacked structures [5]. These observations have been proven to be considerably dependent on the thicknesses of film and substrate. All the above-mentioned investigations are theoretically interpreted within the framework of the traditional two-fluid model (TTF). The TTF [8]–[9] together with the Drude theory describes well the electrodynamics of superconductors. The microwave surface resistance derived in TTF is proportional to operating frequency (log-log scale), which is in good agreement with experimental results. It, however, fails to correctly describe the dependences of surface impedance on temperature, penetration depth and some microscopic parameters, such as the coherence length and electron mean free path. In conventional BCS superconductors, it has been recognized that the electromagnetic response is strongly affected by the coherence effect, a microscopically quantum mechanical result. In order to incorporate the BCS coherence effect, Linden *et al.* [10] have presented the modified two-fluid model (MTF) for calculation of the surface impedance of the conventional low temperature BCS superconductor. It was shown that the microwave surface impedances of conventional superconductors could be accurately described by the MTF.

The purpose of this paper is to comparatively study the multilayer structure made of a conventional low temperature BCS superconducting film on dielectric substrates. We are concerned with the dependence of the effective microwave surface impedance on the BCS coherence factor. We analyzed this electromagnetic propagation-dominated problem on the basis of TTF, MTF, and conventional transmission line theory. The effective surface impedance of the stacked structure in MTF is investigated in parallel with that in TTF. The results of nonresonant and resonant structures are systematically presented and discussed. The intrinsic surface resistance in MTF of superconducting half space is shown to be enhanced considerably compared with TTF. For a superconducting thin film, we find that the intrinsic surface reactance is model-independent, while the surface resistance is closely related to the model considered. In the nonresonant stacked structure, the dielectric substrate at the backside of film only has an effect on the effective surface resistance. In addition, the increase in the thickness of superconducting film will eventually reduce the effective surface impedance to the intrinsic one, namely, the effect of the substrate is completely shielded. As for the resonant stacked structure, the size of resonant peak height in MTF is essentially the same as in TTF. However, the effective surface resistance in MTF is greatly enhanced at

Manuscript received December 12, 1995; revised April 25, 1996. This work was supported by the National Science Council of the Republic of China under Project NSC85-2112-M009-037.

The authors are with the Department of Electronics Engineering and Institute of Electronics, National Chiao-Tung University, Hsinchu, Taiwan, R.O.C.

Publisher Item Identifier S 1051-8223(96)05734-X.

1051–8223/96$05.00 © 1996 IEEE

the nonresonant thickness of the substrate. We successfully interpret the interesting resonance phenomenon by making use of the transverse resonance technique in microwave theory [11].

II. Two-Fluid Theory

The two-fluid theory addresses the microwave property of the superconductor by including two noninteracting fluids: the normal electrons and superconducting electrons. The superconducting electrons manifest themselves as an inductive channel. The normal electrons, however, can be represented by another channel which is both dissipative and inductive. In the microwave regime, the interested frequency is below the superconducting gap frequency, given by $\omega_s = 2\Delta/\hbar$, where Δ is the temperature-dependent gap. The complex ac conductivity of superconductor in TTF is [12]

$$\sigma = \sigma_1 - j\sigma_2 = \sigma_n x_n - j\frac{1}{\mu_0 \omega \lambda_L^2} \tag{1}$$

where the σ_n is the dc normal state conductivity, μ_0 the permeability of free space (taken to be the same as superconductor), ω the angular frequency, x_n the fraction of normal electrons given by

$$x_n = (T/T_c)^4 \equiv t^4 \tag{2}$$

where T_c is the transition temperature of superconductor and t the reduced temperature, and λ_L the temperature-dependent penetration depth given by

$$\lambda_L(T) = \lambda_L(o)/\sqrt{1-t^4}. \tag{3}$$

In obtaining the key result (1), we have used the fact of $\omega\tau \ll 1$, where τ is the momentum relaxation time of normal electron. The TTF (1)–(3) is quite intuitive and analytical so that the microwave response can be quickly numerically illustrated.

As described above, in order to study the microwave properties of BCS superconductors, we may resort to the MTF which encompasses the coherence factor. The MTF combines the accurate merit of microscopic BCS theory, and the nature of speed and intuition in TTF. The coherence factor is reflected on the modification of normal-electron fraction, the result is [10]

$$x_n(T,\omega) = \frac{2\Delta(T)}{k_B T}\exp\left[-\frac{\Delta(T)}{k_B T}\right] \times \ln\left[\frac{\Delta(T)}{\hbar\omega_1}\right]\left[\frac{a}{1+(\omega/\omega_o)^b}+c\right] \tag{4}$$

where gap energy $\Delta(T)$ is approximated by

$$\Delta(T) \approx \Delta_0\left[\cos\left(\frac{\pi}{2}t\right)^2\right]^{\frac{1}{2}}, \tag{5}$$

and $\omega_1 = 1$ rad/s, k_B the Boltzmann constant, $\hbar$ the Planck constant, and material-dependent parameters a, b, c and ω_0. For a typical BCS strong coupling superconductor, Nb ($T_c = 9.2$ K), we find that $a = 0.31$, $b = 0.474$, $c = 0$ and $\omega_0 = 25$ GHz [10]. The temperature and frequency dependences of normal-electron fraction expressed in (4) is reminscent of the results given by Hinken [13] and Kautz [14]. Furthermore, (4) does fit well with the BCS theory.

Equations (1)–(5) provide two alternatives to calculate the microwave surface impedances of superconductors. The TTF is widely used in the analysis of microwave response of high-T_c cuprates [1]–[5]. The MTF, however, is the best candidate for easily investigating the electrodynamic response of BCS superconductors.

III. The Intrinsic and Effective Microwave Surface Impedances of Superconducting Films

A. Surface Impedance of a Semi-Infinite Superconductor

For a semi-infinite superconductor, the surface impedance Z_s is given by

$$Z_s = R_s + jX_s = \left(\frac{j\omega\mu_0}{\sigma}\right)^{1/2} \tag{6}$$

where complex conductivity σ is model-dependent as described in (1), (2) and (4). With the fact of $\sigma_2 \gg \sigma_1$, (6) can be simplified explicitly as

$$R_s = \frac{1}{2}\mu_0^2\omega^2\lambda_L^3\sigma_n x_n, \tag{7}$$

$$X_s = \mu_0\omega\lambda_L. \tag{8}$$

In Figs. 1 and 2, we separately plot the frequency and reduced temperature dependences of R_s of Nb ($T_c = 9.2$ K). For comparative purpose, the results of TTF [x_n in (2)] along with MTF (x_n in (4)) are displayed simultaneously. Fig. 1 evidently elucidates the basic difference in R_s between TTF and MTF. In TTF, the well-known relation of $R_s \sim \omega^2$ is observed, while R_s varies nearly with $\omega^{1.67}$ in MTF because of the inclusion of coherence factors. The discrepancy between MTF and TTF decreases with increasing frequency, especially at higher temperature. The discrepancy shown in Fig. 1 arises from the basic difference in x_n of MTF and TTF. The direct correlation can be seen in the paper of Linden *et al.* [10, Fig. 2]. At a fixed temperature, the difference, x_n(MTF)$-x_n$(TTF), decreases with increasing frequency; however, it essentially is a constant at very low frequency regime. The difference in x_n therefore causes the distinction in R_s as displayed in Fig. 1. Also, the overall surface resistances are enhanced in MTF. All of these features of MTF in Fig. 1 are in good agreement with the experimental reports [10]. Fig. 2 demonstrates the relationship of R_s versus reduced temperature at 10 GHz and 100 GHz. As can be seen, the R_s in MTF is greater than TTF at $t > 0.2$, and eventually coincides at a temperature near T_c. This again can be verified in Fig. 2 of [10]. The

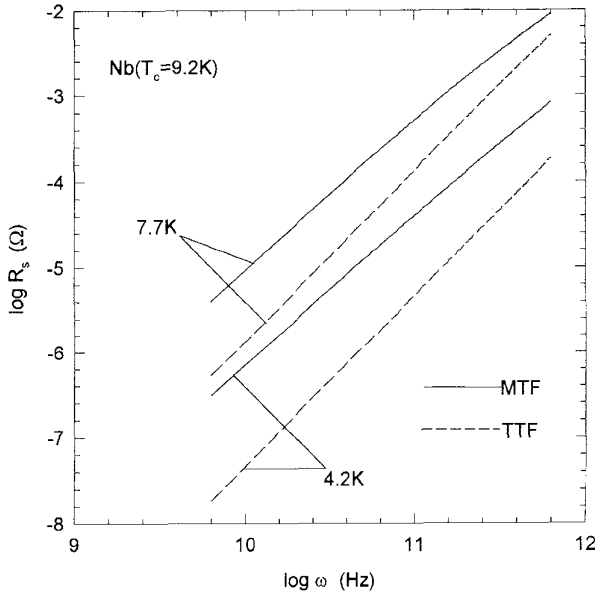

Fig. 1. Calculated surface resistance and reactance in (7) and (8) as a function of angular frequency for both TTF (2) and MTF (4). The material parameters used are $\lambda(0) = 34$ nm, $\sigma_n = (0.31 \times 10^{-8})^{-1}$ s/m, $\Delta_0 = 1.97 k_B T_c$, and $T_c = 9.2$ K for BCS superconductor, Nb [10].

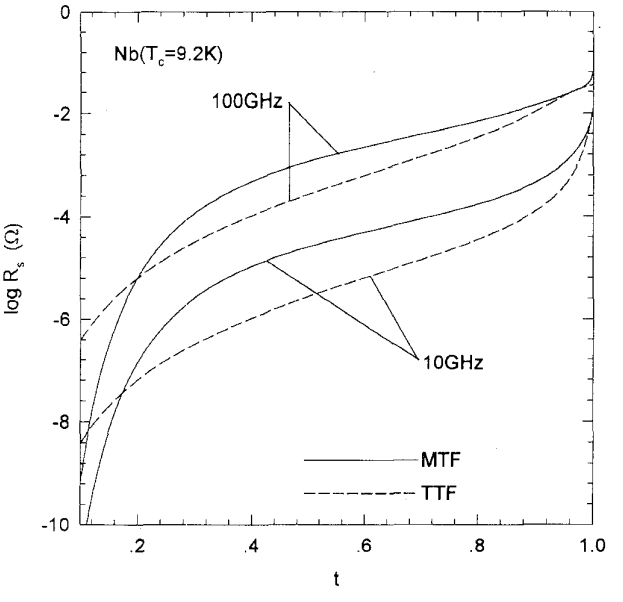

Fig. 2. Calculated surface resistance of bulk superconductor in (7) versus temperature at 10 GHz and 100 GHz for both TTF and MTF. The material parameters used are $\lambda(0) = 34$ nm, $\sigma_n = (0.31 \times 10^{-8})^{-1}$ s/m and $\Delta_0 = 1.97 k_B T_c$ [10].

temperature dependence of x_n shows that the discrepancy, x_n(MTF) − x_n(TTF), increases at $t > 0.2$ and eventually approaches zero at $T \to T_c$. However, at $t < 0.2$, the R_s in MTF is less than TTF. It is also shown that the R_s drops to zero more drastically in MTF. The behavior in R_s for Nb shown in Fig. 2 is essentially in accord with that predicted by another new two-fluid model, the covalent transfer theory (CET) proposed by Dionne [15]. According to the above discussion, the importance and applicability of MTF in interpreting the BCS superconductors should be highly stressed.

B. Intrinsic Surface Impedance of a Superconducting Thin Film

We now switch our attention to BCS superconducting thin film with thickness d. The surface impedance associated to the high frequency response is now referred to as the intrinsic surface impedance, $Z_{s,\text{int}}$, given by [14]

$$Z_{s,\text{int}} = R_{s,\text{int}} + jX_{s,\text{int}} = Z_s \coth(\sqrt{j\omega\mu_o\sigma}\cdot d) \quad (9)$$

where Z_s is described in (6). Simple manipulation leads to

$$R_{s,\text{int}} = \frac{1}{2}\sigma_n\mu_0^2\omega^2\lambda_L^3 x_n\left[\coth(d/\lambda_L) + \frac{d}{\lambda_L}\cdot\text{csch}^2(d/\lambda_L)\right] \quad (10)$$

and

$$X_{s,\text{int}} = \mu_0\omega\lambda_L \coth(d/\lambda_L). \quad (11)$$

In the limit of $d \to \infty$, both (10) and (11) reduces to (7) and (8), respectively. $R_{s,\text{int}}$ is again model-dependent (because of x_n) and $X_{s,\text{int}}$ is essentially independent of the model chosen. By substituting (4) into (10), we have the complete form of $R_{s,\text{int}}$ in MTF, namely,

$$R_{s,\text{int}} = \frac{1}{2}\sigma_n\mu_0^2\omega^2\lambda_L^3\frac{2\Delta}{k_BT}\exp\left(-\frac{\Delta}{k_BT}\right)\ln\left(\frac{\Delta}{\hbar\omega_1}\right) \times\left[\frac{a}{1+(\omega/\omega_0)^b}\right]\left[\coth\left(\frac{d}{\lambda_L}\right)+\frac{d}{\lambda_L}\text{csch}^2\left(\frac{d}{\lambda_L}\right)\right]. \quad (12)$$

The expression (12) reminds us of the surface resistance of a superconductor in the Mattis-Bardeen theory [16]. The surface resistance is

$$R_{s,\text{int}} = \frac{1}{2}\sigma_n\mu_0^2\omega^2\lambda_L^3\frac{2\Delta}{k_BT}\frac{\exp(\Delta/k_BT)}{[1+\exp(\Delta/k_BT)]^2} \cdot\ln\left(\frac{\Delta^*}{\hbar\omega}\right)\left[\coth\left(\frac{d}{\lambda_L}\right)+\frac{d}{\lambda_L}\text{csch}^2\left(\frac{d}{\lambda_L}\right)\right] \quad (13)$$

where Δ^* is given by $\Delta^* = 2.3k_BT + 6k_B^3T^3/\Delta^2$. The similarity in (12) and (13) is expected because the Mattis-Bardeen theory is an approximation of the full BCS theory which is valid either in the extremely dirty limit ($\ell \ll \xi_0$) or the extreme anomalous case ($\xi_0 \gg \lambda_L$), whereas the MTF is a good fit to the BCS theory over a wide range of parameters. However, one should note that the MTF only serves as a good tool for fitting the BCS theory but it is not a replacement of the BCS theory. The application of a Mattis-Bardeen model to a high-T_c superconductor has been considered by Nuss *et al.* [17]. Here, we are concerned with MTF only.

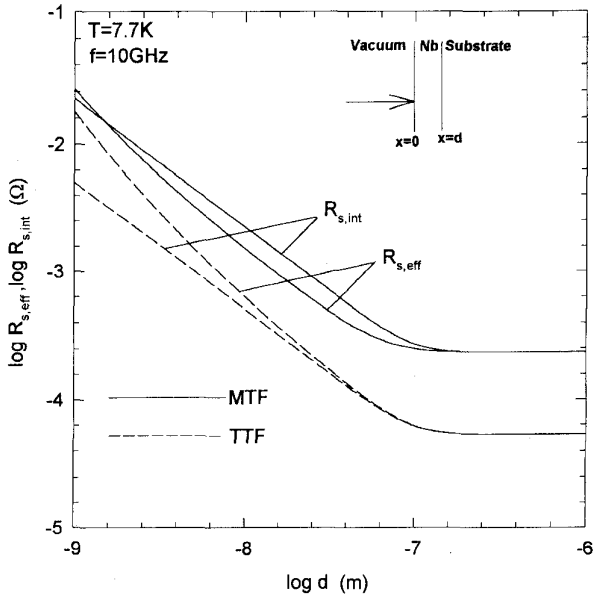

Fig. 3. The intrinsic and effective surface resistances in (10) and (16) as a function of superconducting film thickness at 7.7 K and 10 GHz for both MTF and TTF. The parameters of substrate are described in the text and those of film are the same as shown in Figs. 1 and 2.

C. Effective Surface Impedance of a Superconductor in the Multilayer Structure

Considering the stacked structure depicted in the inset of Fig. 3, the substrate in this structure is assumed to be semi-infinite and the thickness of superconducting film is again taken to be d. A normal incidence TE wave impinges at the plane boundary of a vacuum/superconductor, $x = 0$. The effective surface impedance at $x = 0$ can be found according to the impedance transformation in transmission line theory; that is,

$$Z_{s,\text{eff}} = R_{s,\text{eff}} + jX_{s,\text{eff}} = Z_s \frac{Z_{\text{sub}} + Z_s \tanh(jk_s d)}{Z_s + Z_{\text{sub}} \tanh(jk_s d)}. \quad (14)$$

where Z_{sub} is the wave impedance of the dielectric substrate given by $Z_{\text{sub}} = Z_0/\sqrt{\epsilon_{rs}}$, where Z_0 is the impedance of vacuum in value of 377 Ω, and ϵ_{rs} the relative permittivity of substrate k_s is the complex wavenumber of superconductor defined as

$$k_s \equiv k_s' - jk_s'' = \sqrt{-j\omega\mu_0\sigma} \approx \frac{1}{\lambda_L}\left(\frac{\sigma_1}{2\sigma_2} - j\right) \quad (15)$$

and Z_s is wave impedance of superconductor also described in (6). For thickness of the film, say 1 nm $\leq d \leq$ 10 μm, we can further approximate (14)

$$Z_{s,\text{eff}} = Z_s \coth(\sqrt{j\omega\mu\sigma} \cdot d) + \frac{R_s^2}{Z_{\text{sub}}} \text{csch}^2\left(\frac{d}{\lambda_L}\right). \quad (16)$$

The first term in the right of the above equation indicates the intrinsic impedance $Z_{s,\text{int}}$ of the film as previously described in (9), and the second term relies on the properties of the substrate. Equation (16) clearly reveals that the surface reactance, $X_{s,\text{eff}}$ is equal to $X_{s,\text{int}}$ given in (11). In other words, only the surface resistance is influenced by the dielectric substrate.

Fig. 3 displays the $R_{s,\text{eff}}$ and $R_{s,\text{int}}$ as a function of film thickness. Here, we choose $SrTiO_3$ as the substrate whose permittivity is well described by $\epsilon_{rs} = 2.14 \times 10^3 \cdot [\coth(42/T) - 0.905]^{-1}$ [18]. The numerical results are calculated at the conditions of $T = 7.7$ K and $f = 10$ GHz. It is indicated in this figure that the surface resistances $R_{s,\text{eff}}$ and $R_{s,\text{int}}$ are not only identical but also equal to a constant at film thickness larger than about 160 nm ($\log d \approx -6.8$). It equivalently means that for film thickness larger than 160 nm, the film practically behaves like a bulk material, namely, both $R_{s,\text{eff}}$ and $R_{s,\text{int}}$ reduce to R_s, in (7). This can be qualitatively understood directly from (10) and (16) by taking the limt $d \gg \lambda_L$. It is also shown in this figure that $R_{s,\text{eff}}$ is greater than $R_{s,\text{int}}$ at film thickness less than 100 nm in TTF and the discrepancy is considerable in the very thin film. However, at intermediate film thicknesses the difference between $R_{s,\text{eff}}$ and $R_{s,\text{int}}$ is only appreciable in MTF. Besides, in MTF, the $R_{s,\text{eff}}$ is smaller than $R_{s,\text{int}}$ at about $d \lesssim 100$ nm.

The semi-infinite substrate considered here is of theoretical interest only. Accordingly, we wish to investigate the multilayer structure with finite thickness of substrate which is more useful in the microwave applications.

D. Investigation of Resonant Behavior on Substrates

We take the multilayer structure with substrate thickness of h shown in the inset of Fig. 4 into consideration. By making use of the impedance transformation in succession, we have the effective surface impedance at $x = 0$,

$$Z_{s,\text{eff}} = Z_s \frac{Z_d + Z_s \tanh(jk_s d)}{Z_s + Z_d \tanh(jk_s d)} \quad (17)$$

where the impedance Z_d at $x = d$ is given by

$$Z_d = Z_{\text{sub}} \frac{Z_0 + Z_{\text{sub}} \tanh(jk_{\text{sub}} h)}{Z_{\text{sub}} + Z_0 \tanh(jk_{\text{sub}} h)} \quad (18)$$

where k_{sub} is complex wavenumber in the dielectric slab (assumed to be lossless) and defined as

$$k_{\text{sub}} = k_{\text{sub}}' - jk_{\text{sub}}'' = \omega\sqrt{\mu_0\epsilon_0}\sqrt{\epsilon_{rs}}, \quad (19)$$

and the corresponding substrate wavelength is $\lambda_s = 2\pi/k_{\text{sub}}' = \lambda_0/\sqrt{\epsilon_r}$, where λ_0 is wavelength of free space. Figs 4 and 5 illustrate the effective resistances [real part of (17)] of MTF and TTF as a function of substrate thickness for two film thicknesses at $T = 7.7$ K and $f = 10$ GHz, respectively. The substrate material is $SrTiO_3$. It exhibits a peak in surface resistance at the substrate thickness which is around at the odd multiple of quarter-substrate-wavelength as indicated in these figures. This peak height is essentially the same for both MTF and TTF, but the magnitude of $R_{s,\text{eff}}$ in MTF is higher than in TTF at the nonresonant thicknesses of the substrate. The resonance behavior in the stack structure discussed here is equivalent to a short-circuited transmission line with length being equal to an odd multiple of quarter-substrate-wavelength long or to a parallel lumped

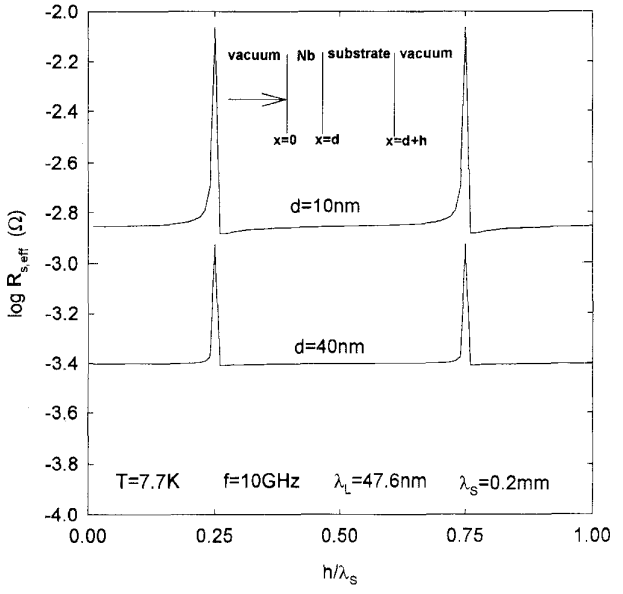

Fig. 4. Calculated effective surface resistance in the real part (17) versus substrate thickness with MTF at various film thicknesses. The parameters are shown inside the figure.

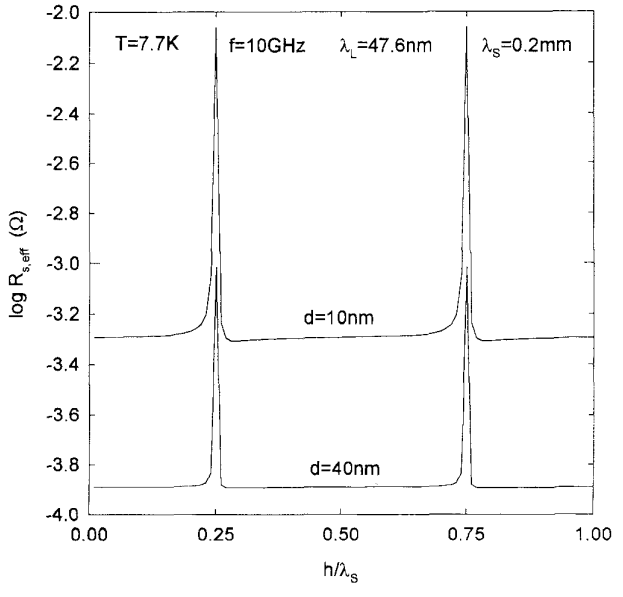

Fig. 5. Calculated effective surface resistance in the real part of (17) versus substrate thickness with TTF at various film thicknesses. The parameters are shown inside the figure.

resonant circuit, as depicted in Fig. 6. The relationships between these two equivalent circuits are $R/L = R_o/L_o$ and $C = C_o\ell/2$ where R_o, L_o and C_o are resistance, inductance and capacitance per unit length of the equivalent transmission line. In this case, the resonance is usually said to be antiresonant [19].

The nature of the substrate resonance phenomenon can be well gained insight with the help of the transverse resonance method (TRM) [11]. At resonance, the microwave field confined inside the substrate slab behaves as a typical standing

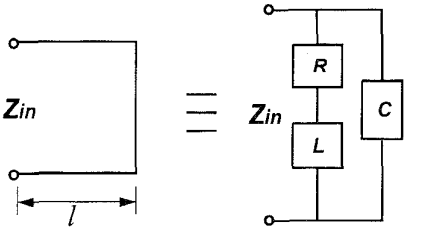

Fig. 6. The equivalent transmission line and lumped circuit resonator.

wave. The impedances of looking backward and forward at $x = d$ can be separately expressed as

$$Z_b(\omega, T, h) = Z_{\text{sub}} \frac{Z_0 + Z_{\text{sub}} \tanh(jk_{\text{sub}}h)}{Z_{\text{sub}} + Z_0 \tanh(jk_{\text{sub}}h)} \tag{20}$$

and

$$Z_f(\omega, T, d) = Z_s \frac{Z_0 + Z_s \tanh(jk_s d)}{Z_s + Z_0 \tanh(jk_s d)} \tag{21}$$

According to the TRM, the resonance occurs at

$$Z_b(\omega, T, h) + Z_f(\omega, T, d) = 0. \tag{22}$$

Equation (22) is actually, in view of (20) and (21), a complex-valued equation with variables h, d, angular frequency ω and temperature T. We can self-consistently check the resonance behavior discussed in Figs. 4–5. By taking appropriate thicknesses for film and substrate, the solution for ω in (22) will, in turn, represent the relevant resonant frequency. Some examples based on MTF are listed below for the purpose of illustrating the solutions for ω in (22).

For $d = 10$ nm,

$$h = \frac{1}{4}\lambda_s \rightarrow \omega = 62.5453 + j0.2872 \text{ (GHz)},$$

$$h = \frac{3}{4}\lambda_s \rightarrow \omega = 62.7360 + j0.0905 \text{ (GHz)}.$$

For $d = 20$ nm,

$$h = \frac{1}{4}\lambda_s \rightarrow \omega = 62.6820 + j0.2771 \text{ (GHz)}$$

$$h = \frac{3}{4}\lambda_s \rightarrow \omega = 62.7818 + j0.0925 \text{ (GHz)}$$

For $d = 40$ nm,

$$h = \frac{1}{4}\lambda_s \rightarrow \omega = 62.7450 + j0.2723 \text{ (GHz)}$$

$$h = \frac{3}{4}\lambda_s \rightarrow \omega = 62.8028 + j0.0909 \text{ (GHz)}.$$

In obtaining the angular frequency, the temperature is taken to be 7.7 K. It is interesting to observe that the frequency is complex-valued. The complex frequency arises from the fact that (22) is mathematically a complex equation mentioned previously. Both the real and imaginary parts indicate their associated significance. The real part of ω listed above represents the resonance frequency which has turn out to be close to 10 GHz ($\omega = 62.8318$ GHz) in good agreement with the results shown in Figs. 4 and 5. On the other hand, the imaginary part of the frequency denotes the loss of the system. The higher it is, the more the loss is. The

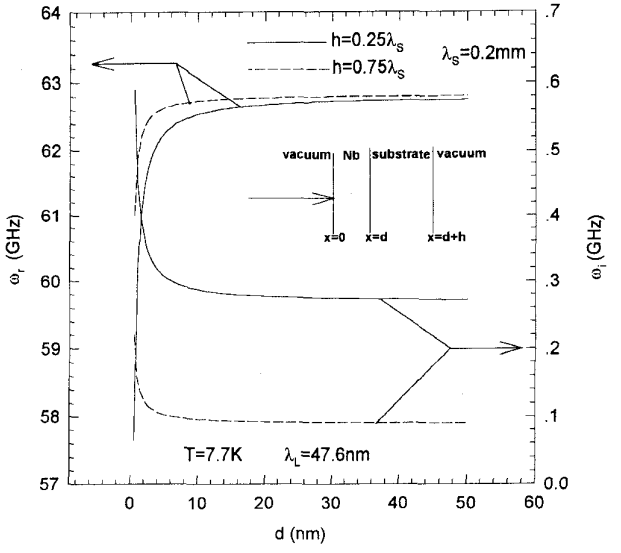

Fig. 7. The real and imaginary parts of complex frequency [solved by (22)] as a function of film thickness at two substrate thicknesses, $d = 0.25\lambda_s,\ 0.75\lambda_s$, with $\lambda_s = 0.2$ mm at a fixed temperature $T = 7.7$ K.

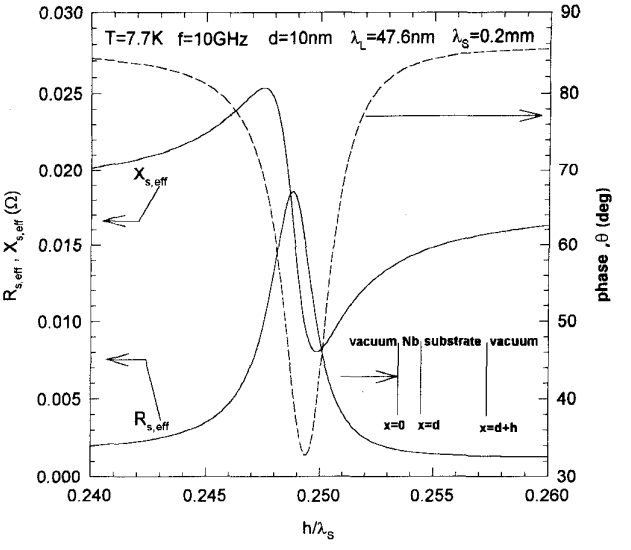

Fig. 8. Calculated effective surface resistance and reactance around the resonant point, $h/\lambda_s = 0.25$. The related parameters are given inside the figure.

overall behaviors of real and imaginary parts of complex frequency versus film thickness are plotted in Fig. 7. The figure shows that the real part, ω_r, drastically decreases for very thin films. At film thickness, $d \gtrsim 10$ nm, the resonance frequency approaches 62.83 GHz, which again reflects the result described previously. The corresponding imaginary frequency ω_i at $d \gtrsim 10$ nm also becomes a constant and increases with decreasing film thickness at about $d < 10$ nm. Also shown is that the increase in substrate thickness will decrease ω_i, namely, the losses are lowered. This can be attributed to the fact that at resonance the dielectric slab acts as a parallel-plate transmission line with thickness h. The transmission line losses are determined by the series resistance together with shunt conductance. The series resistance is essentially independent of substrate thickness. The shunt conductance, however, is inversely proportional to the thickness of the dielectric substrate. Accordingly, the loss will decrease with increasing the substrate thickness.

In Fig. 8 we demonstrate the effective surface resistance, as well as reactance, as a function of substrate thickness around some resonant point. As can be seen, the $X_{s,\text{eff}}$ makes an abrupt transition, from maximum to minimum at resonance. The phase of the impedance defined as $\theta = \tan^{-1}(X_{s,\text{eff}}/R_{s,\text{eff}})$, is also shown in Fig. 8. There is a dip around the resonant position. The deep level is an indication of the extent of the resonance. Fig. 9 indicates the $R_{s,\text{eff}}$ versus h at various film thicknesses near resonant point. The results clearly elucidate the dependence of surface resistance on film thickness. For thicker films, the corresponding resonance-substrate-thickness is closer to quarter wavelength and the peak is also heavily suppressed. One can easily again take advantage of the TRM to self-consistently check the above results.

As a final consideration, let the vacuum at the backside of substrate be replaced by some metal, referred to as ground

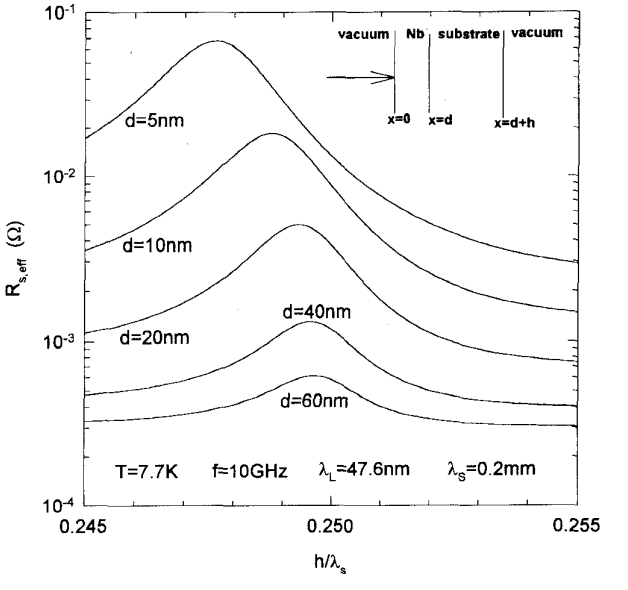

Fig. 9. The effective surface resistance as a function of substrate thickness around the resonant point for various film thicknesses, at $T = 7.7$ K, $f = 10$ GHz.

metal. The resonance-substrate-thickness will become an integer multiple of a half wavelength of the substrate instead of an odd multiple of a quarter wavelength. The shift in substrate thickness can be roughly understood by combining (17) and (18) along with $Z_0 = 0$; namely, the metal is treated as a perfect conductor. The discussion can be found in the work of Hartemann [5]. After substitution of (18) in (17) together with $Z_0 = 0$, the effective surface impedance can be expressed as [5]

$$Z_{s,\text{eff}} = jZ_{\text{sub}} \frac{\tan(k'_{\text{sub}}h) + \frac{2\pi\lambda_L}{\lambda_s}\tanh(d/\lambda_L)}{1 + \frac{\lambda_s}{2\pi\lambda_L}\tanh(d/\lambda_L)\tan(k'_{\text{sub}}h)}. \quad (23)$$

The resonance occurs when the denominator is equal to zero, namely,

$$\tan(k'_{\rm sub}h) = -\frac{2\pi\lambda_L}{\lambda_s}\frac{1}{\tanh(d/\lambda_L)} \approx -2\pi\frac{\lambda_L^2}{\lambda_s d}. \quad (24)$$

With the approximation $\tan x \approx x$ for small x, we can find

$$h \cong n\lambda_s/2 - \lambda_L^2/d, \quad n = \text{integer}. \quad (25)$$

The resonance of substrate thickness h is then near an integral multiple of half wavelengths [5]. However, the argument of Hartemann appears to be questionable. A careful look at (23) reveals that $Z_{s,\rm eff}$ is purely imaginary (if the substrate is lossless) which means a purely reactive behavior in $Z_{s,\rm eff}$. The resonance in surface resistance (resistive behavior) expected by (23) is thus unreasonable. To consider more generally, the complete expression for $Z_{s,\rm eff}$ in (17) can be written as

$$Z_{s,\rm eff} = Z_{\rm sub}\frac{\frac{Z_0}{Z_{\rm sub}}(1-\wedge f(d,h)) + j(\tan(k'_{\rm sub}h) + \wedge\tanh(d/\lambda_L))}{1+\wedge^{-1}f(d,h) + j\frac{Z_0}{Z_{\rm sub}}(\tan(k'_{\rm sub}h) - \wedge^{-1}\tanh(d/\lambda_L))} \quad (26)$$

where $\wedge$ is given by $\wedge \equiv 2\pi\lambda_L/\lambda_s$, and the function $f(d,h)$ is $f(d,h) \equiv \tanh(d/\lambda_L)\tan(k'_{\rm sub}h)$. Equation (26) obviously reduces to (23) in the limit of $Z_0 \to 0$. In the case of $Z_0 \neq 0$, the direct understanding of resonance behavior from (26) is not so obvious. We therefore suggest that this resonance behavior in multilayer structure is best understood from the viewpoint of the transverse resonance method.

IV. Summary

We have systematically examined the surface impedances of superconductors. For BCS superconductors, the coherence effect on microwave response should be taken into account carefully. The simplest fit for a fully microscopic BCS theory within the two-fluid framework is the modified two-fluid model used in this article. Results show considerable enhancement in the surface resistance in MTF but the surface reactance remains the same as TTF. In the layered structure with semi-infinite substrate, the effective surface impedance of the superconductor is decomposed as an intrinsic impedance of finite film thickness and one term related to substrate properties. The effect of a dielectric substrate is only observed in the effective surface resistance instead of effective surface reactance. The inclusion of the BCS coherence effect in MTF evidently increases the intrinsic microwave surface resistance and the effective microwave surface resistance as well. For film thickness greater than some value, such as 160 nm, at $T = 7.7$ K and $f = 10$ GHz, the substrate influence on the structure is fully shielded. The effective surface impedance then reduces to the surface impedance of a bulk superconductor.

In the study of resonance structures, we find the size of resonance peak in surface resistance essentially remains unchanged in MTF and TTF. Nevertheless, the resistance raises to some extent in MTF in the nonresonant region. The resonance point is determined not only by the finite thickness of the dielectric substrate, but also the ground metal. The existence of ground metal at the backside of a dielectric substrate makes the resonance-substrate-thickness be an integral multiple of a half-wavelength instead of an odd multiple of a quarter-wavelength. The resonance result is analyzed by the impedance transform technique and well interpreted with the transverse resonance method. The transverse resonance method introduces a complex frequency. The real part of complex frequency indicates the corresponding resonant frequency which drastically decreases for very thin films, $d \lesssim 10$ nm. However, the imaginary part of complex frequency, increases for $d \lesssim 10$ nm. The imaginary frequency corresponds to the microwave loss of the system and qualitatively consists with the prediction from parallel-plate transmission line. The investigation in multilayer structure presented here provides some possible useful information for the application of a BCS superconducting film in the microwave regime.

References

[1] N. Klein, G. Müller, S. Orbach, H. Piel, H. Chaloupka, B. Roas, L. Schultz, U. Klein, and M. Peiniger, "Millimeter wave surface resistance and London penetration depth of epitaxially grown $YBa_2Cu_3O_{7-x}$ thin films," *Physica C.*, vols. 162–164, pp. 1549–1550, 1989.

[2] N. Klein, H. Chaloupka, G. Müller, S. Orbach, H. Piel, B. Roas, L. Schultz, U. Klein, and M. Peiniger, "The effective microwave surface impedance of high-T_c thin films," *J. Appl. Phys.*, vol. 67, pp. 6940–6945, 1990.

[3] L. Drabeck, K. Holczer, G. Grüner, and D. J. Scalapino, "Ohmic and radiation losses in superconducting films," *J. Appl. Phys.*, vol. 68, pp. 892–894, 1990.

[4] L. Drabeck, K. Holczer, G. Grüner, J. J. Chang, D. J. Scalapino, and T. Venkatesan, "An experimental investigation of $YBa_2Cu_3O_7$ films at millimeter-wave frequencies," *J. Superconduct.*, vol. 3, pp. 317–322, 1990.

[5] P. Hartemann, "Effective and intrinsic surface impedances of high-T_c superconducting thin films," *IEEE Trans. Appl. Superconduct.*, vol. 2, pp. 228–235, 1992.

[6] A. Mogro-Campero, L. G. Turner, A. M. Kadin, and D. S. Mallory, "Film thickness dependence of microwave surface resistance for $YBa_2Cu_3O_7$ thin films," *J. Appl. Phys.* vol. 73, pp. 5295–5297, 1993.

[7] R. Pinto, A. G. Chourey, and P. R. Apte, "Effective surface resistance of $LuBa_2Cu_3O_{7-\delta}$ thin films," *Appl. Phys. Lett.*, vol. 64, pp. 2166–2168, 1994.

[8] C. J. Gorter and H. G. B. Casimir," Superconductivity," *Physica*, vol. 1, pp. 306–310, 1934.

[9] T. Van Duzer and C. W. Turner, *Principles of Superconductive Devices and Circuits*. New York: Elseviser, 1981.

[10] D. S. Linden, T. P. Orlando, and W. G. Lyons, "Modified two-fluid model for superconductor surface impedance calculation," *IEEE Trans. Appl. Superconduct.*, vol. 4, pp. 136–142, 1994.

[11] D. M. Pozar, *Microwave Engineering*. Reading, MA: Addison-Wesley, 1993.

[12] T. P. Orlando and K. A. Delin, *Foundations of Applied Superconductivity*. Reading, MA: Addison-Wesley, 1991.

[13] J. H. Hinken, *Superconductor Electronics: Fundamentals and Microwave Applications*. Berlin: Springer-Verlag, 1988.

[14] R. L. Kautz, "Picosecond pulses on superconducting striplines," *J. Appl. Phys.*, vol. 49, pp. 308–314, 1978.

[15] G. F. Dionne, "New two-fluid superconduction model applied to penetration depth and microwave surface resistance," *IEEE Trans. Appl. Superconduct.*, vol. 3, pp. 1465–1467, 1993.

[16] D. C. Mattis and J. Bardeen, "Theory of the anomalous skin effect in normal and superconducting metals," *Phys. Rev.*, vol. 111, pp. 412–417, 1958.

[17] M. C. Nuss, K. W. Goossen, P. M. Mankiewich, M. L. O'Mally, J. L. Marshall, and R. E. Howard, "Time-domain measurement of the surface resistance of $YBa_2Cu_3O_7$ superconducting film up to 500 GHz," *IEEE Trans. Mag.*, vol. 27, pp. 863–866, 1991.

[18] E. Sawaguchi, A. Kiruchi, and Y. Kodera, "Dielectric constant of strontium titanate at low temperatures," *J. Phys. Soc. Jpn.*, vol. 17, pp. 1666–1667, 1962.

[19] R. E. Collin, *Foundations for Microwave Engineering*. New York: McGraw-Hill, 1992.

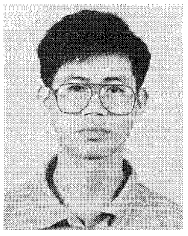

Chien-Jang Wu was born in Taiwan, R.O.C., on March 1, 1962. He received the B. E. degree in electronics engineering, and the M.E. degree in electro-optic engineering from National Chiao Tung University (NCTU), Hsinchu, Taiwan, in 1985 and 1990, respectively. He is now a candidate of Doctoral degree at the College of Electrical Engineering and Computer Science, NCTU.

He was a Liquid-Crystal-Display design engineer at SEIKO EPSON (Taiwan Branch), from 1990 to 1991. He was also a high-frequency hardware engineer at Transystem Inc., Hsinchu, Taiwan, from 1991 to 1992. Since 1993, he has been a Doctoral student at the Institute of Electronics, NCTU. His current interests include the areas of electromagnetic theories together with microwave applications of the high temperature superconductors.

Tseung-Yuen Tseng (M'94-SM'94) received the Ph.D. degree in electroceramics from the School of Materials Engineering, Purdue University, West Lafayette, IN, in 1982.

Before joining National Chiao-Tung University, Hsinchu, Taiwan, R.O.C., in 1983, where he is now a Professor in the Department of Electronics Engineering and the Institute of Electronics, he was briefly associated with the University of Florida. His professional interests are electronic ceramics, ceramic sensors, and high-temperature ceramic superconductors.

Dr. Tseng was nominated for inclusion in the Marquis WHO's WHO in the World in 1996 and is a member of the American Ceramic Society. In 1995 he received a distinguished research award from the National Science Council of the R.O.C. He has published about 100 peer-reviewed technical journal papers and has presented 50 conference papers.